Charge symmetry breaking in light Λ hypernuclei

IOP Conf. Series: Journal of Physics: Conf. Series **966** (2018) 012006 doi:10.1088/1742-6596/966/1/012006

Charge symmetry breaking in light Λ hypernuclei

Avraham Gal[1] **and Daniel Gazda**[2,3]

[1] Racah Institute of Physics, The Hebrew University, 91904 Jerusalem, Israel
[2] Department of Physics, Chalmers University of Technology, SE-412 96 Göteborg, Sweden
[3] Nuclear Physics Institute, 25068 Řež, Czech Republic

E-mail: `avragal@savion.huji.ac.il`

Abstract. Charge symmetry breaking (CSB) is particularly strong in the $A = 4$ mirror hypernuclei ${}^4_\Lambda$H–${}^4_\Lambda$He. Recent four-body no-core shell model calculations that confront this CSB by introducing Λ-Σ^0 mixing to leading-order chiral effective field theory hyperon-nucleon potentials are reviewed, and a shell-model approach to CSB in p-shell Λ hypernuclei is outlined.

1. Introduction

Charge symmetry of the strong interactions arises in QCD upon neglecting the few-MeV mass difference of up and down quarks. With baryon masses of order GeV, charge symmetry should break down at the level of 10^{-3} in nuclei. The lightest nuclei to exhibit charge symmetry breaking (CSB) are the A=3 mirror nuclei ^{3}H–^{3}He, where CSB contributes about 70 keV out of the 764 keV Coulomb-dominated binding-energy difference. This CSB contribution is indeed of order 10^{-3} with respect to the strong interaction contribution in realistic A=3 binding energy calculations, and is also consistent in both sign and size with the scattering-length difference $a_{pp} - a_{nn} \approx 1.7$ fm [1]. It can be explained by $\rho^0\omega$ mixing in one-boson exchange models of the NN interaction, or by considering $N\Delta$ intermediate-state mass differences in models limited to pseudoscalar meson exchanges [2]. In practice, introducing two charge dependent contact interaction terms in chiral effective field theory (χEFT) applications, one accounts quantitatively for the charge dependence of the low energy NN scattering parameters and, thereby, also for the A=3 mirror nuclei binding-energy difference [3]. CSB is manifest, of course, also in heavier nuclei.

In Λ hypernuclei, isospin invariance excludes one pion exchange (OPE) from contributing to ΛN strong-interaction matrix elements. However, it was pointed out by Dalitz and Von Hippel (DvH) that the SU(3) octet $\Lambda_{I=0}$ and $\Sigma^0_{I=1}$ hyperons are admixed in the physical Λ hyperon, thus generating a long-range OPE ΛN CSB potential $V^{\rm OPE}_{\rm CSB}$ [4]. For the mirror ${}^4_\Lambda$H–${}^4_\Lambda$He ground-state (g.s.) levels built on the ^{3}H–^{3}He g.s. cores, and using the DvH purely central wavefunction, the OPE CSB contribution amounts to $\Delta B^{J=0}_\Lambda \approx 95$ keV where $\Delta B^J_\Lambda \equiv B^J_\Lambda({}^4_\Lambda{\rm He}) - B^J_\Lambda({}^4_\Lambda{\rm H})$. This is also confirmed in our present calculations in which tensor contributions add up $\approx$100 keV. Shorter-range CSB meson-mixing contributions appear to be much smaller [5]. Remarkably, the OPE overall contribution of $\approx$200 keV to the CSB splitting of the ${}^4_\Lambda$H–${}^4_\Lambda$He mirror g.s. levels roughly agrees with the large observed g.s. CSB splitting $\Delta B^{J=0}_\Lambda$=233$\pm$92 keV shown in Fig. 1 which is of order 10^{-2} with respect to the Λ nuclear strong interaction contribution in realistic binding energy calculations of the A=4 hypernuclei. Hence, CSB in Λ hypernuclei is likely to be almost one order of magnitude stronger than in ordinary nuclei.

IOP Conf. Series: Journal of Physics: Conf. Series **966** (2018) 012006 doi:10.1088/1742-6596/966/1/012006

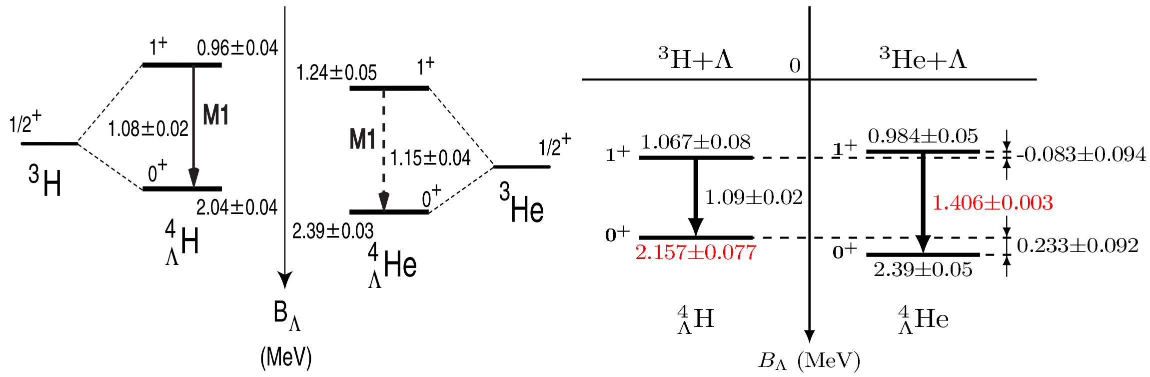

Figure 1. ${}^4_\Lambda$H-${}^4_\Lambda$He level diagram, before (left panel) and after (right panel) the recent measurements of the ${}^4_\Lambda$He excitation energy $E_\gamma(1^+_{\rm exc} \to 0^+_{\rm g.s.})$ at J-PARC [6], and of the ${}^4_\Lambda$H $0^+_{\rm g.s.}$ binding energy at MAMI [7,8], both highlighted in red in the online version. CSB splittings are shown to the very right of the ${}^4_\Lambda$He levels. Figure adapted from [8].

In addition to OPE, $\Lambda - \Sigma^0$ mixing affects also shorter range meson exchanges (e.g. ρ) that in χEFT are replaced by contact terms. Quite generally, in baryon-baryon models that include *explicitly* a charge-symmetric (CS) $\Lambda N \leftrightarrow \Sigma N$ ($\Lambda\Sigma$) coupling, the direct ΛN matrix element of $V_{\rm CSB}$ is obtained from a strong-interaction CS $\Lambda\Sigma$ coupling matrix element $\langle N\Sigma|V_{\rm CS}|N\Lambda\rangle$ by

$$\langle N\Lambda|V_{\rm CSB}|N\Lambda\rangle = -0.0297\,\tau_{Nz}\,\frac{1}{\sqrt{3}}\,\langle N\Sigma|V_{\rm CS}|N\Lambda\rangle, \tag{1}$$

where the z component of the nucleon isospin Pauli matrix $\vec{\tau}_N$ assumes the values $\tau_{Nz} = \pm 1$ for protons and neutrons, respectively, the isospin Clebsch-Gordan coefficient $1/\sqrt{3}$ accounts for the $N\Sigma^0$ amplitude in the $I_{NY} = 1/2$ $N\Sigma$ state, and the space-spin structure of this $N\Sigma$ state is taken identical to that of the $N\Lambda$ state sandwiching $V_{\rm CSB}$. The 3% CSB scale factor -0.0297 in Eq. (1) follows by evaluating the $\Lambda - \Sigma^0$ mass mixing matrix element $\langle\Sigma^0|\delta M|\Lambda\rangle$ from SU(3) mass formulae [4, 9]. The corresponding diagram for generating $\langle N\Lambda|V_{\rm CSB}|N\Lambda\rangle$ is shown in Fig. 2, demonstrating explicitly the δM CSB insertion.

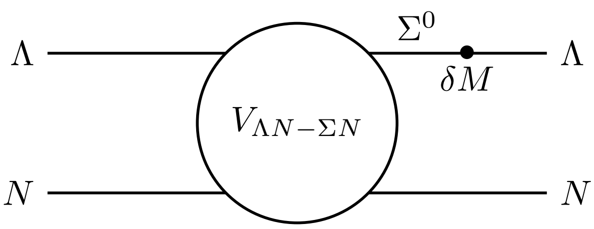

Figure 2. CSB ΛN interaction diagram describing a CS $V_{\Lambda N - \Sigma N}$ interaction followed by a CSB $\Lambda - \Sigma^0$ mass-mixing vertex.

Since the CSB ΛN matrix element in Eq. (1) is given in terms of strong-interaction CS $\Lambda\Sigma$ coupling, one wonders how strong the latter is in realistic microscopic YN interaction models. Recent four-body calculations of ${}^4_\Lambda$He levels [10], using the Bonn-Jülich leading order (LO) χEFT YN CS potential model [11], show that almost 40% of the $0^+_{\rm g.s.} \to 1^+_{\rm exc}$ excitation energy E_x arises from $\Lambda\Sigma$ coupling. This also occurs in the NSC97 models [12] as demonstrated by

IOP Conf. Series: Journal of Physics: Conf. Series **966** (2018) 012006 doi:10.1088/1742-6596/966/1/012006

Akaishi *et al* [13]. With $\Lambda\Sigma$ matrix elements of order 10 MeV, the 3% CSB scale factor in Eq. (1) suggests a CSB splitting $\Delta E_x \sim 300$ keV, in good agreement with the observed splitting $E_{\rm x}({}^4_\Lambda{\rm He})-E_{\rm x}({}^4_\Lambda{\rm H})=$ 320 ± 20 keV [6], see Fig. 1 (right) which also shows a relatively large splitting of the A=4 mirror hypernuclear g.s. levels, $\Delta B_\Lambda^{J=0}$=233±92 keV [7,8], with respect to the ≈70 keV CSB splitting in the mirror core nuclei ^{3}H and ^{3}He.

Here we review recent *ab-initio* no-core shell model (NCSM) calculaions of the A=4 Λ hypernuclei [14,15] using a LO χEFT YN CS interaction model [11] in which CSB is generated by implementing Eq. (1). We also briefly review a shell model approach [9], confronting it with some available data in the p shell.

2. LO χEFT YN interactions

N3LO NN [3] and N2LO NNN interactions [16], both with momentum cutoff $\Lambda = 500$ MeV, are used in our calculations. For hyperons, the Bonn-Jülich SU(3)-based LO YN interaction is used, plus $V_{\rm CSB}$ evaluated from it according to Eq. (1). At LO, V_{YN} consists of regularized pseudoscalar (PS) π, K and η meson exchanges with coupling constants constrained by SU(3)$_{\rm f}$, plus five central interaction contact terms simulating the short range behavior of the YN coupled channel interactions, all of which are regularized with a cutoff momentum $\Lambda \geq m_{\rm PS}$, varied from 550 to 700 MeV. Two of the five contact terms connect ΛN to ΣN in spin-singlet and triplet s-wave channels, and are of special importance for the calculation of CSB splittings. The dominant meson exchange interaction is OPE which couples the ΛN channel exclusively to the $I = \frac{1}{2}$ ΣN channel. K-meson exchange also couples these two YN channels. This $V_{YN}^{\rm LO}$ reproduces reasonably well, with $\chi^2/({\rm d.o.f.}) \approx 1$, the scarce YN low-energy scattering data. It also reproduces the binding energy of ${}^3_\Lambda$H, with a calculated value $B_\Lambda({}^3_\Lambda{\rm H})$=110±10 keV for Λ=600 MeV [17], consistent with experiment (130±50 keV [18]) and with Faddeev calculations reported by Haidenbauer *et al* [19]. Isospin conserving matrix elements of $V_{YN}^{\rm LO}$ are evaluated in a momentum-space particle basis accounting for mass differences within baryon iso-multiplets, while isospin breaking $(I_{NN} = 0) \leftrightarrow (I_{NN} = 1)$ and $(I_{YN} = \frac{1}{2}) \leftrightarrow (I_{YN} = \frac{3}{2})$ transitions are suppressed. The Coulomb interaction between charged baryons is included.

3. NCSM hypernuclear calculations

The NCSM approach to few-body calculations uses translationally invariant harmonic-oscillator (HO) bases expressed in terms of relative Jacobi coordinates [20] in which two-body and three-body interaction matrix elements are evaluated. Antisymmetrization is imposed with respect to nucleons, and the resulting Hamiltonian is diagonalized in a finite HO basis, admitting all HO excitation energies $N\hbar\omega$, $N \leq N_{\rm max}$, up to $N_{\rm max}$ HO quanta. This NCSM nuclear technique was extended recently to light hypernuclei [10, 17]. While it was possible to obtain fully converged binding energies, with keV precision for the A=3 core nuclei ^{3}H and ^{3}He, it was not computationally feasible to perform calculations with sufficiently large $N_{\rm max}$ to demonstrate convergence for ${}^4_\Lambda$H and ${}^4_\Lambda$He. In these cases extrapolation to an infinite model space, $N_{\rm max} \to \infty$, had to be employed. For details see Ref. [15]. We note that ΔB_Λ, and to a lesser extent B_Λ, exhibit fairly weak $N_{\rm max}$ and ω dependence compared to the behavior of absolute energies, and the employed extrapolation scheme was found sufficiently robust. While normally using $N_{\rm max} \to \infty$ extrapolated values based on the last three $N_{\rm max}$ values, it was found that including the last four $N_{\rm max}$ values in the fit resulted in ΔB_Λ values that differed by $\lesssim 10$ keV.

Calculations consisting of fully converged A=3 core binding energies (8.482 MeV for ^{3}H and 7.720 MeV for ^{3}He) and (${}^4_\Lambda$H, ${}^4_\Lambda$He) $0^+_{\rm g.s.}$ and $1^+_{\rm exc}$ binding energies extrapolated to infinite model spaces from $N_{\rm max} = 18(14)$ for $J = 0(1)$ are reported here. The NNN interaction, was excluded from most of the hypernuclear calculations after verifying that, in spite of adding almost 80 keV to the Λ separation energies $B_\Lambda^{J=0}$ and somewhat less to $B_\Lambda^{J=1}$, its inclusion makes a difference of only a few keV for the CSB splittings ΔB_Λ^J in both the $0^+_{\rm g.s.}$ and $1^+_{\rm exc}$ states.

Table 1. CS averages (in MeV) of $B^J_\Lambda(^4_\Lambda\mathrm{H})$ and $B^J_\Lambda(^4_\Lambda\mathrm{He})$ in four-body calculations using LO χEFT YN [11] and NLO χEFT YN [21] interaction models.

	LO (present)	LO [22]	NLO [22]	Exp. (Fig. 1)
$B^{J=0}_\Lambda$	$2.37^{+0.20}_{-0.13}$	2.5 ± 0.1	$1.53^{+0.08}_{-0.06}$	2.27 ± 0.09
$B^{J=1}_\Lambda$	$1.08^{+0.58}_{-0.47}$	$1.4^{+0.5}_{-0.4}$	$0.83^{+0.07}_{-0.10}$	1.03 ± 0.09
$E_\mathrm{x}(0^+_\mathrm{g.s.}\to1^+_\mathrm{exc})$	1.29 ± 0.38	1.05 ± 0.25	0.71 ± 0.04	1.25 ± 0.02

Table 1 lists results obtained for the A=4 hypernuclear levels in the present LO-YN NCSM calculation with V_CSB, and in Nogga's [22] LO- and NLO-YN Faddeev-Yakubovsky calculations without V_CSB. To provide meaningful comparison, the 'present' column lists CS averages over mirror levels in $^4_\Lambda$H and $^4_\Lambda$He. The two LO columns are consistent with each other within the cited uncertainties, which are particularly large for $J = 1$, and both agree with experiment within these uncertainties. Uncertainties reflect the resulting cutoff dependence in the chosen Λ range. The NLO results are almost Λ independent, as inferred from their small uncertainties. However, NLO disagrees strongly with experiment, particularly for $J = 0$ and for the accurately determined E_x. It would be interesting in future work to modify the existing NLO χEFT version [21,22] by refitting the $\Lambda\Sigma$ contact terms to both $B^{J=0,1}_\Lambda$(A=4) CS-averaged values, and then apply the CSB generating equation (1) in four-body calculations of $^4_\Lambda$H–$^4_\Lambda$He.

4. CSB in s-shell hypernuclei

Results of recent four-body NCSM calculations of the A=4 hypernuclei [14,15], using the Bonn-Jülich LO χEFT SU(3)-based YN interaction model [11] with momentum cutoff in the range Λ=550–700 MeV, are shown in Fig. 3. Plotted on the l.h.s. are the calculated $0^+_\mathrm{g.s.} \to 1^+_\mathrm{exc}$ excitation energies in $^4_\Lambda$H and in $^4_\Lambda$He, both of which are found to increase with Λ such that somewhere between Λ=600 and 650 MeV the γ-ray measured values of E_x are reproduced. The $\Lambda - \Sigma^0$ mixing CSB splitting ΔE_x obtained by using Eq. (1) also increases with Λ such that for Λ=600 MeV the calculated value $\Delta E_x = \Delta B^\mathrm{calc}_\Lambda(0^+_\mathrm{g.s.}) - \Delta B^\mathrm{calc}_\Lambda(1^+_\mathrm{exc}) = 330 \pm 40$ keV agrees with the measured value of $E_\mathrm{x}(^4_\Lambda\mathrm{He})-E_\mathrm{x}(^4_\Lambda\mathrm{H})= 320 \pm 20$ keV deduced from Fig. 1 (right).

Plotted on the r.h.s. of Fig. 3 is the $\hbar\omega$ dependence of ΔB^J_Λ, including V_CSB from Eq. (1) and using $N_\mathrm{max} \to \infty$ extrapolated values for each of the four possible B^J_Λ values calculated at cutoff Λ=600 MeV. Extrapolation uncertainties for ΔB^J_Λ are 10 to 20 keV. $\Delta B^{J=0}_\Lambda$ varies over the spanned $\hbar\omega$ range by a few keV, whereas $\Delta B^{J=1}_\Lambda$ varies by up to $\sim$30 keV.

Fig. 3 demonstrates a strong (moderate) cutoff dependence of $\Delta B^{J=0}_\Lambda$ ($\Delta B^{J=1}_\Lambda$):

$$\Delta B^{J=0}_\Lambda = 177^{+119}_{-147}\ \mathrm{keV}, \quad \Delta B^{J=1}_\Lambda = -215^{+43}_{-41}\ \mathrm{keV}. \tag{2}$$

The opposite signs and roughly equal sizes of these ΔB^J_Λ values follow from the dominance of the $^1S_0$ contact term (CT) in the $\Lambda\Sigma$ coupling potential of the LO χEFT YN Bonn-Jülich model [11], whereas the PS SU(3)-flavor octet ($\mathbf{8}_\mathrm{f}$) meson-exchange contributions are relatively small and of opposite sign to that of the $^1S_0$ CT contribution. This paradox is resolved by noting that regularized pieces of Dirac $\delta(\mathbf{r})$ potentials that are discarded in the classical DvH treatment survive in the LO χEFT PS meson-exchange potentials. Suppressing such a zero-range regulated piece of CSB OPE within the full LO χEFT A=4 hypernuclear wavefunctions gives [15]

$$\mathrm{OPE(DvH)}: \quad \Delta B^{J=0}_\Lambda \approx 175 \pm 40\ \mathrm{keV}, \quad \Delta B^{J=1}_\Lambda \approx -50 \pm 10\ \mathrm{keV}, \tag{3}$$

with smaller momentum cutoff dependence uncertainties than in Eq. (2). Both Eqs. (2) and (3) agree within uncertainties with the CSB splittings ΔB^J_Λ marked in Fig. 1.

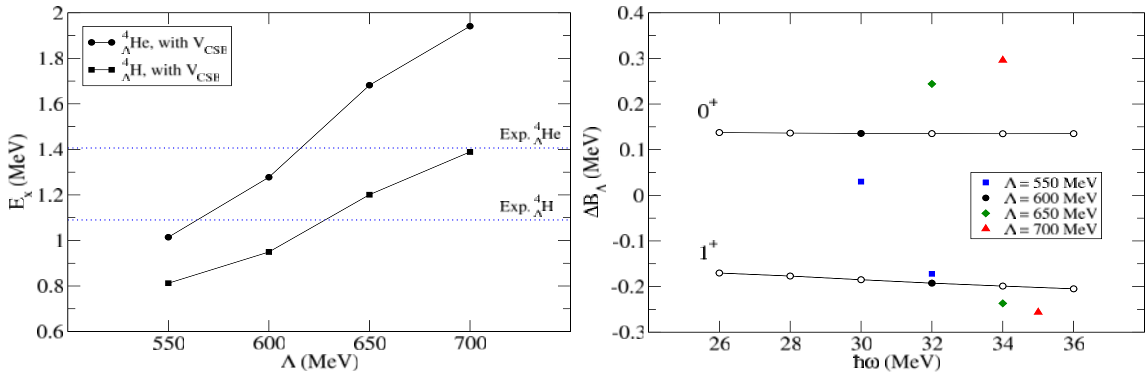

Figure 3. NCSM calculations of $^{4}_{\Lambda}$H and $^{4}_{\Lambda}$He, using CS LO χEFT YN interactions [11] and $V_{\rm CSB}$, Eq. (1), derived from these CS interactions. Left: momentum cutoff dependence of excitation energies $E_{\rm x}(0^+_{\rm g.s.}\to 1^+_{\rm exc})$. The γ-ray measured values of $E_{\rm x}$ from Fig. 1 are marked by dotted horizontal lines. Right: HO $\hbar\omega$ dependence, for Λ=600 MeV, of the separation-energy differences ΔB^J_Λ for $0^+_{\rm g.s.}$ (upper curve) and for $1^+_{\rm exc}$ (lower curve). Results for other values of Λ are shown at the respective absolute variational energy minima. Figure adapted from [15].

5. CSB in p-shell hypernuclei

Recent cluster-model work [23–25] fails to explain CSB splittings in p-shell mirror hypernuclei, apparently for disregarding the underlying CS $\Lambda\Sigma$ coupling potential. In the approach reviewed here, one introduces an effective CS $\Lambda\Sigma$ central interaction $\mathcal{V}_{\Lambda\Sigma} = \bar{V}_{\Lambda\Sigma} + \Delta_{\Lambda\Sigma}\,\vec{s}_N\cdot\vec{s}_Y$, where $\vec{s}_N$ and $\vec{s}_Y$ are the nucleon and hyperon spin-$\frac{1}{2}$ vectors. The p-shell $0p_N 0s_Y$ matrix elements $\bar{V}^{0p}_{\Lambda\Sigma}$ and $\Delta^{0p}_{\Lambda\Sigma}$, listed in the caption to Table 2, follow from the shell-model reproduction of hypernuclear γ-ray transition energies by Millener [26] and are smaller by roughly factor of two than the corresponding s-shell $0s_N 0s_Y$ matrix elements, therefore resulting in smaller Σ hypernuclear admixtures and implying that CSB contributions in the p shell are weaker with respect to those in the $A = 4$ hypernuclei also by a factor of two. To evaluate these CSB contributions, the single-nucleon expression (1) is extended by summing over p-shell nucleons [9]:

$$V_{\rm CSB} = -0.0297\,\frac{1}{\sqrt{3}}\sum_j\,(\bar{V}^{0p}_{\Lambda\Sigma} + \Delta^{0p}_{\Lambda\Sigma}\,\vec{s}_j\cdot\vec{s}_Y)\,\tau_{jz}. \tag{4}$$

Results of applying this effective $\Lambda\Sigma$ coupling model to several pairs of g.s. levels in p-shell hypernuclear isomultiplets are given in Table 2, abridged from Ref. [9]. All pairs except for $A = 7$ are g.s. mirror hypernuclei identified in emulsion [18] where binding energy systematic uncertainties are largely canceled out in forming the listed $\Delta B^{\rm exp}_\Lambda$ values. The B_Λ data selected for the A=7 ($^{7}_{\Lambda}$He, $^{7}_{\Lambda}$Li*, $^{7}_{\Lambda}$Be) isotriplet of lowest $\frac{1}{2}^+$ levels deserve discussion. Recall that the ^{6}Li core state of $^{7}_{\Lambda}$Li* is the 0^+ T=1 at 3.56 MeV, whereas the core state of $^{7}_{\Lambda}$Li$_{\rm g.s.}$ is the 1^+ T=0 g.s. Thus, to obtain $B_\Lambda(^{7}_{\Lambda}{\rm Li}^*)$ from $B_\Lambda(^{7}_{\Lambda}{\rm Li}_{\rm g.s.})$ one makes use of the observation of a 3.88 MeV γ-ray transition $^{7}_{\Lambda}{\rm Li}^* \to \gamma + ^{7}_{\Lambda}$Li [28]. While emulsion $B^{\rm exp}_\Lambda$(g.s.) values [18] were used for the $^{7}_{\Lambda}$Be–$^{7}_{\Lambda}$Li* pair, more recent counter measurements that provide absolute energy calibrations relative to precise values of free-space known masses were used for the $^{7}_{\Lambda}$Li*–$^{7}_{\Lambda}$He pair [27] (FINUDA for $^{7}_{\Lambda}$Li$_{\rm g.s.}$ π^- decay [29] and JLab for $^{7}_{\Lambda}$He electroproduction [30]). Note that the value reported by FINUDA for $B_\Lambda(^{7}_{\Lambda}{\rm Li}_{\rm g.s.})$, 5.85±0.17 MeV, differs from the emulsion value of 5.58±0.05 MeV. Recent B_Λ values from JLab electroproduction experiments for $^{9}_{\Lambda}$Li [31] and $^{10}_{\Lambda}$Be [32] were not used for lack of similar data on their mirror partners.

Table 2. $\langle V_{\rm CSB}\rangle$ contributions (in keV) to $\Delta B^{\rm calc}_{\Lambda}$ in p-shell hypernuclei g.s. isomultiplets, using $\Lambda\Sigma$ coupling matrix elements $\bar{V}^{0p}_{\Lambda\Sigma}$=1.45 MeV and $\Delta^{0p}_{\Lambda\Sigma}$=3.04 MeV in Eq. (4). A similar calculation for the s-shell A=4 mirror hypernuclei [9] is included for comparison. Listed values of $\Delta B^{\rm exp}_{\Lambda}$ are based on g.s. emulsion data [18] except for ${}^{4}_{\Lambda}$He–${}^{4}_{\Lambda}$H [8] and ${}^{7}_{\Lambda}$Li*–${}^{7}_{\Lambda}$He [27].

${}^{A}_{\Lambda}$Z$_>$–${}^{A}_{\Lambda}$Z$_<$	${}^{4}_{\Lambda}$He–${}^{4}_{\Lambda}$H	${}^{7}_{\Lambda}$Be–${}^{7}_{\Lambda}$Li*	${}^{7}_{\Lambda}$Li*–${}^{7}_{\Lambda}$He	${}^{8}_{\Lambda}$Be–${}^{8}_{\Lambda}$Li	${}^{9}_{\Lambda}$B–${}^{9}_{\Lambda}$Li	${}^{10}_{\Lambda}$B–${}^{10}_{\Lambda}$Be
I, J^{π}	$\frac{1}{2}, 0^+$	$1, \frac{1}{2}^+$	$1, \frac{1}{2}^+$	$\frac{1}{2}, 1^-$	$1, \frac{3}{2}^+$	$\frac{1}{2}, 1^-$
$\langle V_{\rm CSB}\rangle$	232	50	50	119	81	17
$\Delta B^{\rm calc}_{\Lambda}$	226	−17	−28	+49	−54	−136
$\Delta B^{\rm exp}_{\Lambda}$	233±92	−100±90	−20±230	+40±60	−210±220	−220±250

The $\langle V_{\rm CSB}\rangle$ p-shell entries listed in Table 2 were calculated with Λ-hypernuclear weak-coupling shell-model wavefunctions in terms of nuclear-core g.s. leading SU(4) supermultiplet components, except for $A = 8$ where the first excited nuclear-core level had to be admixed in. The listed $A = 7-10$ values of $\langle V_{\rm CSB}\rangle$ exhibit strong SU(4) correlations, highlighted by the enhanced value of 119 keV for the SU(4) nucleon-hole configuration in ${}^{8}_{\Lambda}$Be–${}^{8}_{\Lambda}$Li with respect to the modest value of 17 keV for the SU(4) nucleon-particle configuration in ${}^{10}_{\Lambda}$B–${}^{10}_{\Lambda}$Be. This enhancement follows from the relative magnitudes of the Fermi-like interaction term $\bar{V}^{0p}_{\Lambda\Sigma}$ and its Gamow-Teller partner term $\Delta^{0p}_{\Lambda\Sigma}$. Noting that both the $A = 4$ and $A = 8$ mirror hypernuclei correspond to SU(4) nucleon-hole configuration, the roughly factor two ratio of $\langle V_{\rm CSB}\rangle_{A=4}$=232 keV to $\langle V_{\rm CSB}\rangle_{A=8}$=119 keV reflects the approximate factor of two for $0s_N0s_Y$ to $0p_N0s_Y$ $\Lambda\Sigma$ matrix elements discussed above. However, in distinction from the A=4 g.s. isodoublet where $\Delta B_{\Lambda} \approx \langle V_{\rm CSB}\rangle$, the increasingly negative Coulomb contributions in the p-shell overcome the positive $\langle V_{\rm CSB}\rangle$ contributions, with ΔB_{Λ} becoming negative definite for $A \geq 9$.

Comparing $\Delta B^{\rm calc}_{\Lambda}$ with $\Delta B^{\rm exp}_{\Lambda}$ in Table 2, we note the reasonable agreement reached between the $\Lambda\Sigma$ coupling model calculation and experiment for all five pairs of p-shell hypernuclei listed here. Extrapolating to heavier hypernuclei, one might naively expect negative values of $\Delta B^{\rm calc}_{\Lambda}$. However, this assumes that the negative Coulomb contribution remains as large upon increasing A as it is in the beginning of the p shell, which need not be the case. As nuclear cores beyond $A = 9$ become more tightly bound, the Λ hyperon is unlikely to compress these nuclear cores as much as it does in lighter hypernuclei, so that the additional Coulomb repulsion in ${}^{12}_{\Lambda}$C, for example, over that in ${}^{12}_{\Lambda}$B may not be sufficiently large to offset the attractive CSB contribution to $B_{\Lambda}({}^{12}_{\Lambda}{\rm C})-B_{\Lambda}({}^{12}_{\Lambda}{\rm B})$, in agreement with the value 50±110 keV suggested recently for this A=12 B_{Λ}(g.s.) splitting using FINUDA and JLab counter measurements [27]. In making this argument one relies on the expectation, based on SU(4) supermultiplet fragmentation patterns in the p shell, that $\langle V_{\rm CSB}\rangle$ does not exceed ∼100 keV.

Some implications of the state dependence of CSB splittings, e.g. the large difference between the calculated $\Delta B_{\Lambda}(0^+_{\rm g.s.})$ and $\Delta B_{\Lambda}(1^+_{\rm exc})$ in the s shell, Eqs. (2) or (3), are worth noting also in the p shell. The most spectacular one concerns the ${}^{10}_{\Lambda}$B g.s. doublet splitting, where adding the $\Lambda\Sigma$ coupling model CSB contribution of ≈ -27 keV to the ≈110 keV CS $1^-_{\rm g.s.} \to 2^-_{\rm exc}$ g.s. doublet excitation energy calculated in this model [26] helps bring it down well below 100 keV, which is the upper limit placed on it from past searches for a $2^-_{\rm exc} \to 1^-_{\rm g.s.}$ γ-ray transition [33,34].

6. Summary and Outlook

The recent J-PARC E13-experiment observation of a 1.41 MeV ${}^{4}_{\Lambda}{\rm He}(1^+_{\rm exc} \to 0^+_{\rm g.s.})$ γ-ray transition [6], and the recent MAMI-A1 determination of $B_{\Lambda}({}^{4}_{\Lambda}{\rm H})$ to better than 100 keV [7,8], plus the recenly approved J-PARC E63 experiment to remeasure the ${}^{4}_{\Lambda}\mathrm{H}(1^{+}_{\rm exc} \to 0^{+}_{\rm g.s.})$ γ-ray transition, arose renewed interest in the sizable CSB already confirmed thereby in the A=4 mirror hypernuclei. It was shown in the present report how a relatively large $\Delta B_{\Lambda}(0^{+}_{\rm g.s.})$ CSB contribution of order 250 keV, in rough agreement with experiment, arises in ab-initio four-body calculations [14, 15] using χEFT YN interactions already at LO.

In p-shell hypernuclei, a $\Lambda\Sigma$ coupling shell-model approach was shown to reproduce CSB splittings of g.s. binding energies [9]. More theoretical work in this mass range, and beyond, is needed to understand further and better the salient features of $\Lambda\Sigma$ dynamics [35]. On the experimental side, the recently proposed (π^{-}, K^{0}) reaction [36] should be explored, in addition to the standard (π^{+}, K^{+}) reaction, in order to study simultaneously two members of a given Λ hypernuclear isomultiplet, for example reaching both ${}^{12}_{\Lambda}\mathrm{B}$ and ${}^{12}_{\Lambda}\mathrm{C}$ on a carbon target.

Acknowledgments

A.G. acknowledges instructive discussions with John Millener, as well as the gracious hospitality extended by the organizers of SPRING 2017 at Ischia, Italy. The research of D.G. was supported by the Grant Agency of the Czech Republic (GACR), Grant No. P203/15/04301S.

References

[1] Miller G A, Opper A K and Stephenson E J 2006 *Annu. Rev. Nucl. Part. Sci.* **56** 253
[2] Machleidt R and Müther H 2001 *Phys. Rev.* C **63** 034005
[3] Entem D R and Machleidt R 2003 *Phys. Rev.* C **68** 041001(R)
[4] Dalitz R H and Von Hippel F 1964 *Phys. Lett.* **10** 153
[5] Coon S A, Han H K, Carlson J and Gibson B F 1999 *Meson and Light Nuclei '98* ed J Adam, P Bydžovský, J Dobeš, R Mach and J Mareš (Singapore: WS) pp 407-413
[6] Yamamoto T O *et al* (J-PARC E13 Collaboration) 2015 *Phys. Rev. Lett.* **115** 222501
[7] Esser A *et al* (MAMI A1 Collaboration) 2015 *Phys. Rev. Lett.* **114** 232501
[8] Schulz F *et al* (MAMI A1 Collaboration) 2016 *Nucl. Phys.* A **954** 149
[9] Gal A 2015 *Phys. Lett.* B **744** 352
[10] Gazda D, Mareš J, Navrátil P, Roth R and Wirth R 2014 *Few-Body Syst.* **55** 857
[11] Polinder H, Haidenbauer J and Meißner U -G 2006 *Nucl. Phys.* A **779** 244
[12] Rijken Th A, Stoks V G J and Yamamoto Y 1999 *Phys. Rev.* C **59** 21
[13] Akaishi A, Harada T, Shinmura S and Myint K S 2000 *Phys. Rev. Lett.* **84** 3539
[14] Gazda D and Gal A 2016 *Phys. Rev. Lett.* **116** 122501
[15] Gazda D and Gal A 2016 *Nucl. Phys.* A **954** 161
[16] Navrátil P 2007 *Few-Body Syst.* **41** 117
[17] Wirth R, Gazda D, Navrátil P, Calci A, Langhammer J and Roth R 2014 *Phys. Rev. Lett.* **113** 192502
[18] Davis D H 2005 *Nucl. Phys.* A **754** 3c
[19] Haidenbauer J, Meißner U -G, Nogga A and Polinder H 2007 *Topics in Strangeness Nuclear Physics* ed P Bydžovský, J Mareš and A Gal (New York: Springer) *Lecture Notes in Physics* **724** pp 113-140
[20] Navrátil P, Kamuntavičius G P and Barrett B R 2000 *Phys. Rev.* C **61** 044001
[21] Haidenbauer J, Petschauer S, Kaiser N, Meißner U -G, Nogga A and Weise W 2013 *Nucl. Phys.* A **915** 24
[22] Nogga A 2013 *Nucl. Phys.* A **914** 140 and references to earlier works cited therein
[23] Hiyama E, Yamamoto Y, Motoba T and Kamimura M 2009 *Phys. Rev.* C **80** 054321
[24] Zhang Y, Hiyama E and Yamamoto Y 2012 *Nucl. Phys.* A **881** 288
[25] Hiyama E and Yamamoto Y 2012 *Prog. Theor. Phys.* **128** 105
[26] Millener D J 2012 *Nucl. Phys.* A **881** 298 and references listed therein
[27] Botta E, Bressani T and Feliciello A 2017 *Nucl. Phys.* A **960** 165
[28] Tamura H *et al* 2000 *Phys. Rev. Lett.* **84** 5963
[29] Agnello M *et al* (FINUDA Collaboration and Gal A) 2009 *Phys. Lett.* B **681** 139
[30] Gogami T *et al* (JLab HKS Collaboration) 2016 *Phys. Rev.* C **94** 021302(R)
[31] Urciuoli G M *et al* (JLab Hall A Collaboration) 2015 *Phys. Rev.* C **91** 034308
[32] Gogami T *et al* (JLab HKS Collaboration) 2016 *Phys. Rev.* C **93** 034314
[33] Chrien R E *et al* 1990 *Phys. Rev.* C **41** 1062
[34] Tamura H *et al* 2005 *Nucl. Phys.* A **754** 58c
[35] Gal A and Millener D J 2013 *Phys. Lett.* B **725** 445
[36] Agnello M, Botta E, Bressani T, Bufalino S and Feliciello A 2016 *Nucl. Phys.* A **954** 176